

Multimodal transition and stochastic antiresonance in squid giant axons

L. S. Borkowski

Faculty of Physics, Adam Mickiewicz University, Umultowska 85, 61-614 Poznan, Poland

(Received 16 March 2010; published 13 October 2010)

The experimental data of Takahashi *et al.* [*Physica D* **43**, 318 (1990)], on the response of squid giant axons stimulated by periodic sequence of short current pulses is interpreted within the Hodgkin-Huxley model. The minimum of the firing rate as a function of the stimulus amplitude I_0 in the high-frequency regime is due to the multimodal transition. Below this singular point only odd multiples of the driving period remain and the system is sensitive to noise. The coefficient of variation has a maximum and the firing rate has a minimum as a function of the noise intensity, which is an indication of the stochastic coherence antiresonance. The model calculations reproduce the frequency of occurrence of the most common modes in the vicinity of the transition. A linear relation of output frequency vs I_0 above the transition is also confirmed.

DOI: 10.1103/PhysRevE.82.041909

PACS number(s): 87.19.ln, 87.19.lc, 87.19.lb

The Hodgkin-Huxley (HH) model [1] is a prototypical resonant neuron with the main resonant frequency typically of order 40–60 Hz. Its output interspike intervals (ISI) can be classified in terms of integer multiples of the driving period. The multimodality is revealed when the HH neuron is stimulated by noisy inputs, such as additive noise [2,3], random synaptic inputs [2,4,5], or channel noise [6]. Such ISI histograms are encountered frequently in periodically forced sensory neurons. An explanation in terms of a two-state system with noise was put forward by Longtin *et al.* [7]. The multimodal character is manifest also in a deterministic HH model near excitation threshold [8,9] and in regimes of irregular response between mode-locked states [9]. It was shown recently that also the parity of ISI plays a significant role [10]. Even (odd) modes dominate in the vicinity of even (odd) mode-locked states. The most significant manifestation of this effect is the multimodal odd-all transition between states 3:1 and 2:1 [10], where the coefficient of variation (C_V) has a maximum and the firing rate has a minimum. The notation $p:q$ means q output spikes for every p input current pulse. Below this singularity only odd multiples of the input period exist, and above it harmonics of both parities participate in the response. The transition may be crossed by varying either the stimulus amplitude or the input period. The minimum of the firing rate occurs slightly above the transition.

In earlier experiments in giant axons of squid stimulated periodically by a train of short rectangular current pulses, the firing rate, defined as the ratio of the output and input frequencies f_o/f_i , had a well pronounced minimum as a function of the interval between adjacent pulses [11] or the stimulus amplitude [12]. On careful inspection of results of Ref. [12] one may notice that even modes were absent below the minimum. This effect occurred near the excitation threshold, between states 3:1 and 2:1. Another interesting result was the continuous relation between the firing rate and the stimulus amplitude. This set of experimental and theoretical results deserves a more detailed comparison.

The theory can be tested also by considering a periodic drive in the presence of noise. Noisy biological systems [2,5,13–16], including the HH neuron, are known to exhibit stochastic resonance. This phenomenon is mainly, although not exclusively, characterized by a maximum of the signal-to-noise ratio as a function of the noise intensity. Another

effect associated with the presence of noise is the decrease in the firing threshold and the coherence resonance [17,18], where the minimum variability of the output signal, expressed by C_V in the absence of a deterministic drive, is achieved at some intermediate noise strength. Recently it was found experimentally [19,20] and theoretically [21,22] that small amplitude noise may decrease the firing rate or even turn it off. The nonlinear system in the vicinity of the multimodal transition is a natural candidate for finding interesting effects due to noise since the trajectories of different modes are very close in parameter space. In the following we compare experimental data to theoretical results for the deterministic case and calculate the system's response to a periodic drive with additive Gaussian noise.

In the experiment of Takahashi *et al.* [12] the squid axon was stimulated by periodic train of rectangular current steps of width equal to 0.3 ms. Figure 1 shows the experimentally obtained firing rate as a function of stimulus amplitude scaled by the minimum current threshold I_t . On the left side of the minimum only odd modes were recorded. Even modes were present at the minimum point, with the 6:1 mode occurring more frequently than the 4:1 component, and 2:1 entirely absent. This is consistent with calculation results [10], where even modes disappear before reaching the multimodal transition (which is slightly below the minimum of the firing rate), with the low-order modes vanishing first, beginning with mode 2:1.

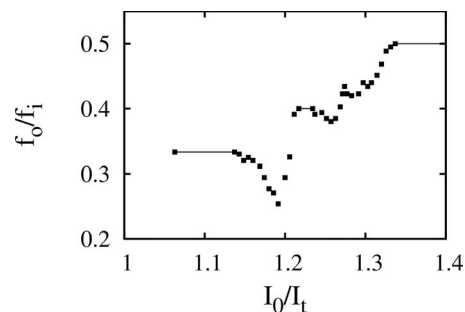


FIG. 1. The average firing rate f_o/f_i as a function of the stimulus amplitude I from the work of Takahashi *et al.* [12]. I_t is the minimum current threshold obtained in the range $T_i=2.5$ ms to $T_i=6.5$ ms. The measurements were carried out at $T_i=3.8$ ms.

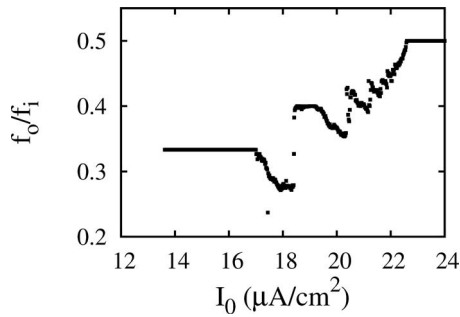


FIG. 2. The calculated average firing rate at $T_i=7$ ms without noise.

We try to reproduce this type of dependence using the HH model with the classic parameter set and rate constants [1],

$$C \frac{dV}{dt} = -I_{Na} - I_K - I_L + I_{app}, \quad (1)$$

where I_{Na} , I_K , I_L , and I_{app} are the sodium, potassium, leak, and external currents, respectively. $C=1 \mu\text{F}/\text{cm}^2$ is the membrane capacitance. The input current is a periodic set of rectangular steps of width equal to 0.6 ms and height I_0 . Equations are integrated within the fourth-order Runge-Kutta scheme with a time step of 0.001 ms. The data points are obtained from runs of 400 s, discarding the initial 4 s. The dependence of the firing rate on the stimulus amplitude is shown in Fig. 2, where the input period is $T_i=7$ ms. The similarity to experiment is striking. Although the calculated minimum occurs at almost twice the experimental T_i , the other time scales such as the refractory period and the time span of the bifurcation diagram differ by a similar factor. The entire dynamics of the axon from the study of Takahashi *et al.* is significantly faster than that of Hodgkin and Huxley. This difference of time scales is not unusual. Long time ago Best [23] noted that the axon used by Hodgkin and Huxley was of poor quality, and in later studies significantly higher conductivities were obtained. Paydarfar *et al.* [19] in their recent study recorded firing periods in the range between 7 and 16 ms. The overall dynamics of Figs. 1 and 2 agrees very well, including the location and depth of the local minima. We verified that the form of Fig. 2 was unchanged for pulse widths between 0 and 1 ms after dividing the current amplitude by $\int_0^{T_i} I(t) dt$.

Figure 3 shows the response diagram in the high-frequency limit. The dotted line separates the monostable firing solution from the silent state and bistable areas where the limit cycle coexists with a fixed-point solution. Boundaries of bistability were determined using a continuation method starting from a region with a single solution.

The experimental local maximum on the plateau $f_o/f_i=0.4$ is due to the state 10/100, where modes 2:1 and 3:1 alternate. The other local maximum at $f_o/f_i=0.429$ with tendency to lock into the $(10)^2/100$ state was also reproduced. Figure 4 shows the relative frequency of participation of the most common modes on a logarithmic scale. Higher-order modes appear more frequently near the minimum of the firing rate. Experimental and calculated ISI histograms are

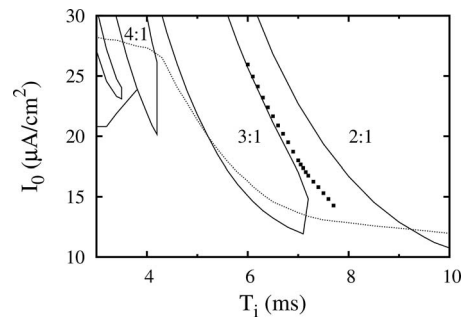


FIG. 3. The bifurcation diagram in the T_i - I_0 plane, showing the main mode-locked states in the model without noise. The unmarked intrusion in the upper left corner is the 5:1 state. The bottom part of the figure is occupied by the silent state. In the firing part of the diagram there are two solutions below the dotted line (see, e.g., the tip of the 3:1 and 4:1 states). Here, the limit cycle coexists with the fixed point. The average firing rate is a continuous function of I_0 at the excitation threshold between 4 and 5 ms and between 7.2 and 9 ms. The average firing rate is a continuous function of I_0 . Full squares show the location of the minima of the firing rate. The borders of states below $T_i=4.5$ ms are shown in an approximate form. The detailed picture is less regular and somewhat more complex.

compared in Table I. The overall agreement is quite remarkable. Also the calculated evolution of individual modes as a function of I_0 is close to measured values. In experiment the probability of appearance of mode 4:1 between $I_0/I_t=1.2$ and 1.3 remains in the range 0.06–0.08, which agrees well with Fig. 4 for I_0 between 18 and 22 $\mu\text{A}/\text{cm}^2$. The published experimental runs [12] contain 80–100 output spikes for selected data points. On the basis of this data set we can conclude that the frequency of participation of the low-order modes is approximately reproduced in simulations. Above

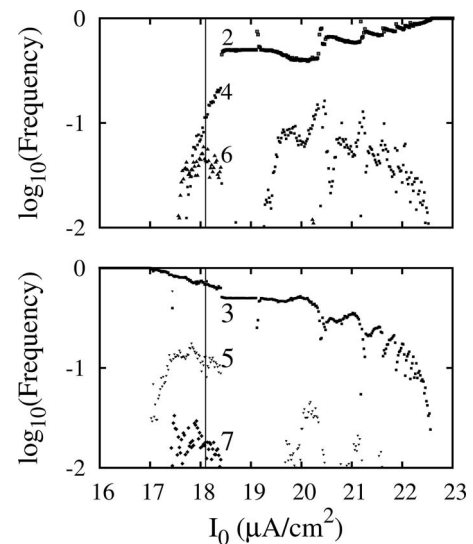


FIG. 4. The relative frequency of occurrence of low-order even (upper) and odd (lower) modes for the parameter set of Fig. 2. Numbers 2,3,... indicate modes 2:1,3:1,..., respectively. The vertical line marks the position of the minimum of the firing rate. Odd modes disappear below approximately $I_0=17.5 \mu\text{A}/\text{cm}^2$.

TABLE I. Frequency of occurrence of the six lowest modes at the minimum of the firing rate. The upper row is based on Fig. 13(e) from the experimental data of Takahashi *et al.* [12]. The bottom row is the result of calculations, assuming $T_i=7$ ms and $I_0=18 \mu\text{A}/\text{cm}^2$ (see Fig. 4).

Mode					
2	3	4	5	6	7
0	0.66	0.04	0.12	0.09	0.04
0.002	0.74	0.07	0.11	0.04	0.02

the multimodal transition the experimental firing rate near the threshold rises linearly with the stimulus amplitude (see Fig. 5). The dependence of f_o/f_i on I_0 is well reproduced in Fig. 6, except in the vicinity of the 2:1 plateau, where an addition of a small amount of noise would improve the fit.

We now consider the model with a Gaussian white noise:

$$C \frac{dV}{dt} = -I_{Na} - I_K - I_L + I_{app} + C\xi(t), \quad (2)$$

where $\langle \xi_i(t) \rangle = 0$, $\langle \xi_i(t)\xi_j(t') \rangle = 2D\delta(t-t')$, and D is expressed in mV^2/ms . The HH equations are integrated using the second-order stochastic Runge-Kutta algorithm [24]. The simulations are again carried out with the time step of 0.001 ms and are run for 400 s, discarding the initial 4 s.

There is a tendency to assume that biological systems, including neurons, should always be treated as noisy systems. While the neuron is sensitive to noise, it is not obvious that single neuron dynamics should always include stochastic terms. Figure 7 shows the quick disappearance of the $f_o/f_i=0.4$ plateau in Fig. 2 with increasing noise. Comparing with the experimental data in Fig. 1 we conclude that calculations reproduce experimental data only for $D < 10^{-4}$. Certainly more experiments are needed to understand the role of noise in neurons.

The odd-all transition is preserved under small levels of noise. Figure 8 shows the relative participation of the lowest modes for the current amplitude range from Fig. 4. The histograms of higher-order modes near the transition are smoothed out, but their edges and maxima remain almost unchanged.

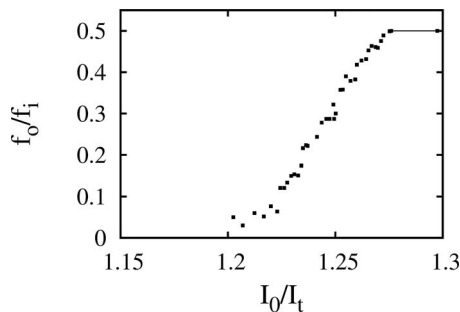


FIG. 5. The linear relation of the firing rate vs the stimulus amplitude above the multimodal transition point at $T_i=4$ ms. These are experimental results of Takahashi *et al.* [12].

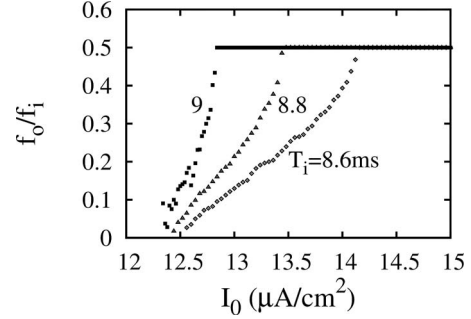


FIG. 6. Calculated average firing rate vs stimulus amplitude above the multimodal transition for three values of T_i . The current pulse width is 0.6 ms.

Figure 9 (upper) presents the firing rate as a function of D for three parameter sets from the 3:1 plateau of Fig. 2. On the deterministic response diagram in Fig. 3 these points are located above the dotted line. For small noise f_o/f_i drops quickly below 1/3 over an entire plateau, with the biggest drop near the edges. This behavior should be contrasted with the resonant regime where the central part of each plateau maintains phase locking over much larger range of noise intensities, and $D \sim 1$ is needed to lower the firing rate of an entire plateau below the $D=0$ value [9]. Another difference is the direction of frequency changes at the plateau edges. In the resonant state the frequency below (above) the plateau midpoint is lowered (increased) [9]. In the antiresonant limit the entire plateau is unstable to a small noise which slows down the system considerably.

C_V as a function of D has a maximum for the same parameter set (see lower diagram of Fig. 9). The increased variability is associated with increased participation of higher-order modes and may be called a *stochastic coherence antiresonance*.

A maximum of C_V was found earlier in a leaky integrate-and-fire model with an absolute refractory period for suprathreshold base current [25]. A small local maximum of C_V at intermediate noise level was also found by Luccioli *et al.* [5] in a HH model driven by a dc current, where the neuron was stimulated by a large number of stochastic inhibitory and excitatory postsynaptic potentials. It was pointed out that the stochastic antiresonance may exist in regions of bistability [22], when the stable limit cycle coexists with other attrac-

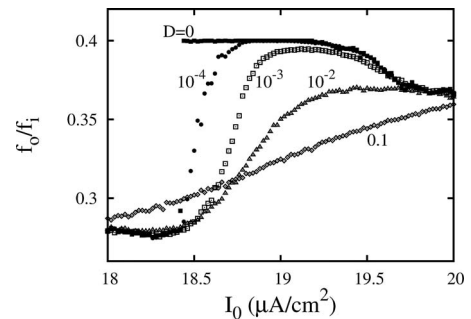


FIG. 7. Sensitivity of the $f_o/f_i=0.4$ plateau from Fig. 2 to noise. The location of the minimum of the firing rate remains almost unchanged up to $D \approx 10^{-2}$.

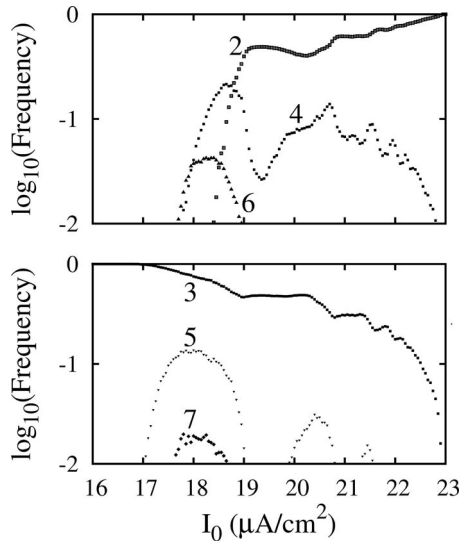


FIG. 8. The relative frequency of occurrence of low-order even (upper) and odd (lower) modes for the parameter set of Fig. 2 and in the presence of small Gaussian noise, $D=0.001$.

tors. This typically occurs in the vicinity of a bifurcation when the value of the bifurcation parameter slightly exceeds the critical value. In the HH model near the multimodal transition there are many competing limit cycles. Noise enhances trajectory switching and may even stop the firing entirely. A decrease in the firing rate and an increase in incoherence may occur along much of the excitation threshold, where the deterministic system is bistable or responds irregularly [9].

In conclusion, numerical solutions of the deterministic HH equations show that the minimum of the firing rate observed by Takahashi *et al.* [12] is due to the multimodal transition [10]. The statistics of the experimental spike trains confirm that below the transition only odd modes remain. Even modes are present at the minimum of f_o/f_i , in agreement with theoretical calculations [10]. The calculated frequencies of occurrence of the most common modes are close to experimental values. Also the location of the minimum of f_o/f_i in the vicinity of the 3:1 state is consistent with the simulations. The linear rise of the output frequency as a function of the stimulus strength above the multimodal transition was also confirmed. The excitation threshold in the antiresonant limit is higher by about a factor of 2 compared to the resonant regime. The rise of threshold for frequencies of current pulses exceeding the resonant frequency was observed experimentally by Kaplan *et al.* [26].

Further support for the significance of the parity of the modes comes from the experiment of Paydarfar *et al.* [19], who found that the quiescent periods between highly regular bursts were always equal to even multiples of the resonant period. An ISI histogram with odd modes was obtained by Racicot and Longtin [27] in a chaotically forced FitzHugh-

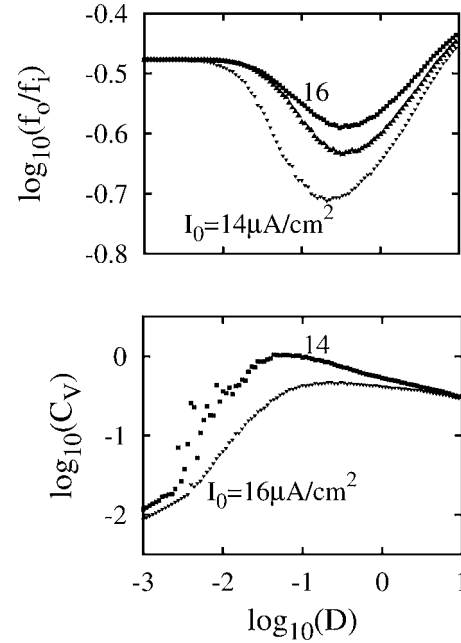


FIG. 9. The firing rate (upper) and the coefficient of variation (lower) as functions of the noise intensity at $T_i=7$ ms. The middle curve in the upper diagram was obtained for $I_0=15 \mu\text{A}/\text{cm}^2$. At $D=0$ all three curves start in the 3:1 mode. The maximum of the coefficient of variation as a function of the noise intensity is a property of the stochastic coherence antiresonance. The maximum of C_V and the minimum of the firing rate occur at different noise levels. The irregularity of the $I_0=14 \mu\text{A}/\text{cm}^2$ curve is a consequence of proximity to the excitation threshold.

Nagumo (FHN) model. FHN equations are often used as a substitute for the full HH model. It would therefore be useful to investigate whether the main features of the odd-all ISI transition are reproduced in the FHN model with deterministic and stochastic drives.

Perturbing the system with noise changes significantly the f vs I_0 dependence, eliminating the local minima. However the deepest minimum of this curve survives up to $D \approx 10^{-2}$. In the regime below the multimodal transition the 3:1 plateau disappears rapidly for small noise. The firing rate has a minimum and C_V has a maximum as a function of the noise intensity. These predictions are expected to be valid for short stimuli of different shapes and can be tested experimentally. The multimodal transition and the accompanying stochastic antiresonance are important for the understanding of excitable systems. The intermediate minimum of the firing rate in the Hodgkin-Huxley model is due to the competition of modes of opposite parities. Similar effects may occur in other dynamical systems with a well-defined resonance.

Computations were performed in the Computer Center of the Tri-city Academic Computer Network in Gdansk.

- [1] A. L. Hodgkin and A. F. Huxley, *J. Physiol. (London)* **117**, 500 (1952).
- [2] P. H. E. Tiesinga, J. V. José, and T. J. Sejnowski, *Phys. Rev. E* **62**, 8413 (2000).
- [3] B. Agüera y Arcas, A. L. Fairhall, and W. Bialek, *Neural Comput.* **15**, 1715 (2003).
- [4] D. Brown, J. Feng, and S. Feerick, *Phys. Rev. Lett.* **82**, 4731 (1999).
- [5] S. Luccioli, T. Kreuz, and A. Torcini, *Phys. Rev. E* **73**, 041902 (2006).
- [6] P. Rowat, *Neural Comput.* **19**, 1215 (2007).
- [7] A. Longtin, A. Bulsara, and F. Moss, *Phys. Rev. Lett.* **67**, 656 (1991).
- [8] J. R. Clay, *J. Comput. Neurosci.* **15**, 43 (2003).
- [9] L. S. Borkowski, *Nonlinear Dynamics of Hodgkin-Huxley Neurons* (Adam Mickiewicz University Press, Poznan, 2010).
- [10] L. S. Borkowski, *Phys. Rev. E* **80**, 051914 (2009).
- [11] G. Matsumoto, K. Aihara, Y. Hanyu, N. Takahashi, S. Yoshizawa, and J. Nagumo, *Phys. Lett. A* **123**, 162 (1987).
- [12] N. Takahashi, Y. Hanyu, T. Musha, R. Kubo, and G. Matsumoto, *Physica D* **43**, 318 (1990).
- [13] K. Wiesenfeld and F. Moss, *Nature (London)* **373**, 33 (1995).
- [14] B. Doiron, A. Longtin, N. Berman, and L. Maler, *Neural Comput.* **13**, 227 (2000).
- [15] W. C. Stacey and D. M. Durand, *J. Neurophysiol.* **86**, 1104 (2001).
- [16] M. Rudolph and A. Destexhe, *J. Comput. Neurosci.* **11**, 19 (2001).
- [17] Hu Gang, T. Ditzinger, C. Z. Ning, and H. Haken, *Phys. Rev. Lett.* **71**, 807 (1993).
- [18] A. S. Pikovsky and J. Kurths, *Phys. Rev. Lett.* **78**, 775 (1997).
- [19] D. Paydarfar, D. B. Forger, and J. R. Clay, *J. Neurophysiol.* **96**, 3338 (2006).
- [20] C. K. Sim and D. B. Forger, *J. Biol. Rhythms* **22**, 445 (2007).
- [21] B. S. Gutkin, J. Jost, and H. C. Tuckwell, *EPL* **81**, 20005 (2008).
- [22] B. S. Gutkin, J. Jost, and H. C. Tuckwell, *Naturwiss.* **96**, 1091 (2009).
- [23] E. N. Best, *Biophys. J.* **27**, 87 (1979).
- [24] R. L. Honeycutt, *Phys. Rev. A* **45**, 600 (1992).
- [25] B. Lindner, L. Schimansky-Geier, and A. Longtin, *Phys. Rev. E* **66**, 031916 (2002).
- [26] D. T. Kaplan, J. R. Clay, T. Manning, L. Glass, M. R. Guevara, and A. Shrier, *Phys. Rev. Lett.* **76**, 4074 (1996).
- [27] D. M. Racicot and A. Longtin, *Physica D* **104**, 184 (1997).